

Heat shock protein (HSP)90 involvement in the development of idiopathic epiretinal membranes

This is the peer reviewed version of the following article:

Original:

Tosi, G.M., Regoli, M., Altera, A., Galvagni, F., Arcuri, C., Bacci, T., et al. (2020). Heat shock protein (HSP)90 involvement in the development of idiopathic epiretinal membranes. INVESTIGATIVE OPHTHALMOLOGY & VISUAL SCIENCE, 61(8), 1-9 [10.1167/iovs.61.8.34].

Availability:

This version is available <http://hdl.handle.net/11365/1111768> since 2020-10-01T20:34:51Z

Published:

DOI: <http://doi.org/10.1167/iovs.61.8.34>

Terms of use:

Open Access

The terms and conditions for the reuse of this version of the manuscript are specified in the publishing policy. Works made available under a Creative Commons license can be used according to the terms and conditions of said license.

For all terms of use and more information see the publisher's website.

(Article begins on next page)

Heat Shock Protein 90 Involvement in the Development of Idiopathic Epiretinal Membranes

Gian Marco Tosi,¹ Mari Regoli,² Annalisa Altera,^{2,5} Federico Galvagni,³ Cataldo Arcuri,⁴ Tommaso Bacci,¹ Ines Elia,³ Giulia Realini,³ Maurizio Orlandini,³ and Eugenio Bertelli²

¹Department of Medicine, Surgery and Neuroscience, University of Siena, Siena, Italy

²Department of Molecular and Developmental Medicine, University of Siena, Siena, Italy

³Department of Biotechnology, Chemistry and Pharmacy, University of Siena, Siena, Italy

⁴Department of Experimental Medicine, University of Perugia, Perugia, Italy

⁵Department of Life Sciences, University of Siena, Siena, Italy

Correspondence: Eugenio Bertelli, Department of Molecular and Developmental Medicine, University of Siena, Via Aldo Moro 2, 53100 Siena, Italy; eugenio.bertelli@unisi.it

GMT and MR equally contributed to the work.

Received: December 31, 2019

Accepted: June 22, 2020

Published: July 27, 2020

Citation: Tosi GM, Regoli M, Altera A, et al. Heat shock protein 90 involvement in the development of idiopathic epiretinal membranes. *Invest Ophthalmol Vis Sci*. 2020;61(8):34. <https://doi.org/10.1167/iovs.61.8.34>

PURPOSE. This work was aimed to further characterize cells of idiopathic epiretinal membranes (iERMs). We wanted to determine the contribution of 90-kDa heat shock protein (HSP90) to sustain the transforming growth factor- β (TGF- β)-mediated signal transduction pathway in iERM.

METHODS. Immunofluorescence and confocal microscopy were carried out on deplasticized sections from 36 epiretinal membranes processed for electron microscopy and on frozen sections from five additional samples with antibodies against α -smooth muscle actin (α SMA), vimentin, glial fibrillary acidic protein (GFAP), SMAD2, HSP90 α , type-II TGF- β 1 receptor (T β RII), type-I collagen, and type-IV collagen. In addition, Müller MIO-M1 cells were transfected with HSP90 and challenged with TGF- β 1.

RESULTS. Double and triple labeling experiments showed that a variable number of T β RII⁺ cells were present in 94.1% of tested iERMs and they were mostly GFAP⁻/ α SMA⁺/vimentin⁺/HSP90 α ⁺. In almost half of the cases these cells contained type-I collagen, suggesting their involvement in matrix deposition. HSP90 overexpressing MIO-M1 cells challenged with TGF- β 1 showed increased levels of T β RII, SMAD2, SMAD3, and phosphor-SMAD2. Nuclear SMAD2 staining could be observed in HSP90 α ⁺ cells on frozen sections of iERMs.

CONCLUSIONS. Cells in iERMs that express T β RII are also HSP90 α ⁺ and show the antigenic profile of myofibroblast-like cells as they are GFAP⁻/ α SMA⁺/vimentin⁺. HSP90 α -overexpressing MIO-M1 cells challenged with TGF- β 1 showed an increased activation of the SMAD pathway implying that HSP90 α might play a role in sustaining the TGF- β 1-induced fibrotic response of iERM cells.

Keywords: epiretinal membranes, macular puckers, MIO-M1 cells, HSP90, TGF- β

Idiopathic epiretinal membranes (iERMs) are fibrocellular sheets of tissue that develop on the vitreoretinal interface of the eye. When located in front of the fovea and having a retracting behavior, they generate a clinical condition known as macular pucker, which disrupts the underlying retinal architecture strongly affecting visual capacity.¹

Components of iERMs are cells and extracellular matrix. As far as cells are concerned, it is still not clear which cell lineage they derive from. Ultrastructural and immunocytochemical investigations based on the expression of specific cell markers have pointed to hyalocytes, Müller cells, astrocytes, fibroblasts, and retinal pigmented epithelial cells as the ultimate source of epiretinal membrane (ERM) cells.²⁻⁴ When considering iERMs, molecular markers appear mixed up probably because of an ongoing process of transdifferentiation. Thus for instance, coexpression of glial fibrillary acidic protein (GFAP) with hyalocyte markers has been reported,^{4,5} and α -smooth muscle actin (α SMA) is a constant

finding even though cells that supposedly generate ERMs do not express it in a resting state. Whichever the cell type of origin is, de novo expression of α SMA likely testifies a transdifferentiation progression toward a myofibroblastic phenotype.^{4,6-9} Transdifferentiation into myofibroblast-like cells is probably the key event for the production of collagen proteins and for the generation of the force required for ERM retraction.^{9,10} Interestingly, α SMA can be expressed by cells derived from retinal pigment epithelial cells and hyalocytes, respectively, after a process of epithelial-mesenchymal transition or transdifferentiation,^{4,11,12} and by Müller cells^{13,14} after a process of glial-mesenchymal transition.¹⁵ In practice, all cell types that have been proposed to give rise to ERM cells can transdifferentiate into a myofibroblast-like phenotype because reactive astrocytes can also express α SMA.¹⁶

ERMs contain variable amounts of extracellular matrix. Components of the extracellular matrix identified so far include type-I to VI collagens, heparan sulfate

proteoglycans, laminin, fibronectin, tenascin, and decorin.^{4,17–22} Hence ERMs have the major hallmarks of fibrotic disorders as they show an exuberant deposition of extracellular matrix and/or the development of a retracted fibrotic scar tissue, which eventually disrupts organ architecture and function.²³ Molecules mediating fibrosis are numerous and some of them have been found in ERMs as well. Transforming growth factor- β (TGF- β) is one of them, as immunohistochemistry demonstrated the expression of both TGF- β 1 and its receptor in cells of iERMs.⁷ TGF- β 1 binding to type-II TGF- β receptor (T β RII) activates type-I TGF- β receptor, which in turn triggers SMAD-dependent and SMAD-independent signal transduction pathways.²⁴ Both pathways eventually promote transcription of TGF- β target genes that are needed for fibrogenesis. SMAD proteins are cytoplasmic mediators of the canonical TGF- β signal pathway. Activation of the SMAD-dependent pathway requires SMAD2 and SMAD3 phosphorylation. Once phosphorylated, SMAD 2/3 binds to SMAD4 and move to the nucleus to regulate gene expression including *COL1A1* (type-I collagen).²⁵ TGF- β 1 signaling pathway can be modulated by numerous molecules, one of them being the 90-kDa heat shock protein (HSP90). HSP90 is a family of proteins that act as chaperones for several client proteins. Their role in fibrotic disorders has been shown in a number of experimental contexts employing specific inhibitors.^{26–28} As the use of HSP90 inhibitors is a promising therapeutic approach for fibrosis²⁹; HSP90 is currently the focus of intense research. Here we report that HSP90 α can be found in samples of iERMs and that its expression appears to be correlated with the presence of T β RII and α SMA. Because there are evidences that at least part of ERM cells may derive from Müller cells,^{9,21} we also explored the mechanisms underlying HSP90 modulation of the TGF- β 1-induced transduction pathway in MIO-M1 cells, a spontaneously immortalized human Müller cell line.¹³

MATERIALS AND METHODS

Patients and Samples

Patients affected by iERMs were subjected to primary 25-gauge pars plana vitrectomy (PPV) by the same surgeon (GMT) without intraocular complications between January 2014 and August 2017 at the Ophthalmology Section of Siena University Hospital, Siena, Italy. The exclusion criteria were diabetes mellitus, coexisting ocular disorders, except cataract; patients requiring PPV for indications other than those mentioned earlier; and patients previously subjected to intraocular surgery, except cataract surgery. The research adhered to the principles of the Declaration of Helsinki, and the institutional review board approved the study. Patients were treated after being informed of the nature of the treatment being offered, its potential risks, benefits, adverse effects, possible outcomes, and after having signed a consent form. ERMs were stained based on surgeon preference and were excised using a Grieshaber Revolution forceps (Alcon Laboratories Inc., Fort Worth, TX, USA). ERM peeling was always started from the edge of the macula. Fluid/air exchange was performed in every patient at the end of the procedure. In cases with coexisting cataract, phacoemulsification and intraocular lens implantation was performed before vitrectomy through a corneal incision.

A total number of 36 iERMs, 15 of them associated with the internal limiting membrane (ILM), were included in this

study, and processed as follows. Membranes were fixed with 1.25% glutaraldehyde in 0.1 M sodium cacodylate for 24 hours at 4°C and postfixed in 1% OsO₄ for 2 hours at 4°C. After fixation, samples were dehydrated and embedded in Epon following standard procedures. Semithin sections (1- μ m thick), cut from each block of resin with an ultramicrotome Ultratome Nova (LKB, Bromma, Sweden), were placed on well-degreased slides.

Five additional iERMs were sampled between September and December 2019. They were embedded in OCT and frozen in isopentane prechilled with liquid nitrogen as previously reported.³⁰ Seven-micrometer thick sections were cut and stored at -80°C until used for immunofluorescence experiments.

Antibodies

The following primary antibodies were used: goat anti- α SMA (code SAB2500963), mouse anti- β -actin (code A5441), mouse anti-FLAG (code F-4042), and monoclonal mouse anti-vimentin (clone V9; code V6389) that were from Sigma-Aldrich (Saint Louis, MO, USA); rabbit anti-human GFAP (code 18-0063) and rabbit anti-human SMAD2 (code 51-1300) that were from Zymed (San Francisco, CA, USA); monoclonal mouse anti-GFAP (clone 6F2; code M0761) was purchased from DAKO (Glostrup, Denmark); rabbit anti-HSP90 α (code MA3-010) was received from ThermoFisher (Rockford, IL); rabbit anti-human T β RII (code sc-220) was obtained from Santa Cruz Biotechnology (Dallas, TX, USA); goat anti-vimentin was a kind gift from Peter Traub (Max-Planck Institut für Zellbiologie, Rosenhof, Ladenburg, Germany)³¹; rabbit anti-human type-I collagen was purchased from Novus Biologicals (Littleton, CO, USA), and goat anti-human type-IV collagen was obtained from SouthernBiotech (Birmingham, AL, USA); rabbit anti-phosphoSMAD2 (code 3108), anti-SMAD2 (code 5339), and anti-SMAD3 (code 9523) were purchased from Cell Signaling Technologies (Carlsbad, CA, USA); biotinylated rabbit anti-histone H3 (code NB500-171B) was received from Novus Biologicals LLC (Centennial, CO, USA).

The secondary antibodies, all double-labeling grade, were donkey tetramethylrhodamine (TRITC)-conjugated anti-goat IgG (code AP180R) from Chemicon (Temecula, CA, USA), donkey Cy2-conjugated F(ab')₂ fragment anti-rabbit IgG (code 711-226-152), donkey Cy5-conjugated F(ab')₂ fragment anti-rabbit IgG (code 711-176-152), and donkey Cy5-conjugated F(ab')₂ fragment anti-mouse IgG (code 715-176-150) from Jackson ImmunoResearch Laboratories (West Grove, PA, USA).

Immunofluorescence and Confocal Microscopy

Confocal microscopy was carried out on semithin sections. Immunoreactions were performed on resin removal and antigen retrieval as previously reported.²² Positive immunoreactions were unveiled with the appropriate secondary antibodies conjugated with FITC or Cy2, TRITC, and Cy5. The combination of primary antibodies employed were the following: (1) goat anti- α SMA and rabbit anti-GFAP; (2) goat anti- α SMA, rabbit anti-GFAP, and mouse anti-vimentin; (3) rabbit anti-T β RII, goat anti-vimentin, and mouse anti-GFAP; (4) rabbit anti-T β RII, mouse anti-HSP90 α , and goat anti- α SMA; (5) rabbit anti-GFAP, mouse anti-vimentin, and goat anti- α SMA; (6) goat anti-type IV collagen, rabbit anti-type I collagen, and mouse anti-vimentin;

and (7) goat anti- α SMA, rabbit anti-type I collagen, and mouse anti-HSP90 α . Once images were acquired with the confocal microscope to visualize cell nuclei, some experiments were continued, and the coverslips were gently removed. Antibodies were stripped incubating slides in 0.1 M glycine, pH 2.51, at 50°C for 30 minutes, and sections were reprobed overnight with biotin-conjugated anti-histone H3 antibody followed by Rhodamine Red-X-conjugated streptavidin (Jackson ImmunoResearch Laboratories). A clear nuclear staining was achieved, and new images were acquired on the previously spotted regions of interest. Images acquired exactly on the same microscopic fields (those with cytoplasmic labeling and those with the nuclear staining) were superimposed with Adobe Photoshop CS3 software (Adobe, San Jose, CA).

Expression of GFAP, α SMA, and vimentin was evaluated in all samples with the exception of three membranes that were too damaged to make a proper judgement over cell staining. In addition, T β RII expression, HSP90-immunoreactive cells, and type-I containing cells were assessed respectively in 17, 20, and 24 randomly chosen iERMs. Frozen sections were fixed in 10% buffered formalin, permeabilized with 0.1% Triton X-100 in PBS for 10 minutes and incubated overnight with the anti-SMAD2 antibody. After washing, sections were challenged with Cy2-conjugated anti-rabbit IgG, anti-HSP90 α antibody, TRITC-conjugated anti-mouse IgG, and finally nuclei were counterstained with TO-PRO-3 iodide DNA dye (Invitrogen, Carlsbad, CA, USA).

Controls were carried out following the same earlier mentioned procedures with the exception of the primary antibodies that were replaced with PBS or with nonimmune serum from the same animal species employed to raise the antibodies.

Images were acquired with an LSM510 Zeiss (Carl Zeiss, Jena, Germany) confocal microscope with selective multi-tracking excitation.

Cell Culture, Lentiviral Particles Production, Cell Transduction, Whole Cell Extracts, and Immunoblotting

Spontaneously immortalized human Müller glia cell line MIO-M1, kindly provided at passage #15 by GA Limb from the Institute of Ophthalmology and Moorfield Eye Hospital (London, UK),¹³ was grown in Dulbecco's modified Eagle's medium containing high glucose and glutamine, and supplemented with 10% fetal bovine serum. Cells were amplified and frozen at passage #17 for subsequent experiments. For each transduction experiment, cells were thawed and employed within passage #19. Under normal culture conditions, MIO-M1 cells express markers of mature Müller cells, including cellular retinaldehyde binding protein, glutamine synthetase, vimentin, and epidermal growth factor receptor at least until passage #45.¹³ Lentiviral particles production and cell transduction were performed as previously described³² with the following modifications: Lenti-X 293T (Takara Bio, Shiga, Japan) packaging cells were transiently transfected with the TransIT-VirusGEN Transfection Reagent (Mirus Bio LLC, Madison, WI, USA) following the manufacturer's instructions. MIO-M1 cells were transduced with lentiviral vectors for the expression of FLAG-tagged human HSP90 (Cat #: RC218420L1; OriGene, Rockville, MD, USA) or the Green Fluorescent Protein (GFP) as negative control and

control of infection efficiency. GFP and HSP90-FLAG transfected cells were treated with 1 ng/mL human recombinant TGF- β 1 (Cat #: 240-B; R&D Systems, Inc., Minneapolis, MN, USA) for the indicated time points (ranging from 2–24 hours), washed with PBS and lysed. Protein extracts and immunoblotting were performed as previously described.³³ Western blot shown is representative of three separate experiments.

RESULTS

T β RII is Expressed in GFAP[−]/ α SMA⁺/Vimentin⁺ ERM Cells

Semithin sections of iERMs were first labeled with antibodies to GFAP, α SMA, and vimentin, and results from these initial experiments are summarized in Table 1. GFAP-expressing cells were present in 78.8% of samples (26 iERMs), and were barely detectable in 9.1% of membranes (3 iERMs). GFAP was apparently absent in 12.1% of cases (4 iERMs). However, α SMA-expressing cells were found in 97% of samples (32 iERMs), and they were very few in 3% of cases (1 iERM). In contrast, vimentin was found in all iERMs and labeled virtually all cells. The ratio between α SMA⁺ and GFAP⁺ cells could be estimated only with good approximation. As summarized in Table 2, most iERMs (60.6% of samples) were characterized by a great majority of α SMA⁺ cells, whereas only one iERM was formed mainly by GFAP⁺ cells.

Analysis in double and triple labeling experiments showed that α SMA- and GFAP-expressing cells were mostly different cells which, however, coexpressed vimentin as well (Figs. 1A–H). GFAP and α SMA, however, were not mutually exclusive molecular markers as a minor population of rare double labeled cells could be found in all samples provided with both GFAP- and α SMA-expressing cells (Figs. 1I–K). From the results of this set of experiments, we could infer that the great majority of all vimentin⁺/GFAP[−] and vimentin⁺/ α SMA[−] cells were respectively α SMA-expressing and GFAP-expressing cells.

Expression of T β RII was found in all tested iERMs but one (94.1% of cases). The number of positive cells was variable according to the sample. Triple labeling with anti-T β RII, anti-vimentin, and anti-GFAP antibodies showed that the receptor was mainly located in vimentin⁺/GFAP[−] cells (Figs. 2A–H), which based on the previous consideration, should be considered mostly as α SMA⁺ cells. Also few vimentin⁺/GFAP⁺ cells, however, were labeled by the anti-T β RII antibody (Figs. 2A–D).

T β RII⁺ Cells also Express HSP90 α

To further characterize ERM cells, we also stained sections with antibodies anti-HSP90 α . HSP90 α fluorescence could be detected with variable intensity in 75% of iERMs, being undetectable only in 4 samples out of 20. Triple labeling experiments showed that HSP90 α colocalized with α SMA in T β RII⁺ cells (Figs. 2I–L).

HSP90 α Immunoreactivity is Stronger in GFAP[−] Cells and Type-I Collagen is Found within HSP90 α ⁺/Vimentin⁺/ α SMA⁺ Cells

HSP90 α immunoreactivity, however, was not restricted to just α SMA⁺ cells. Indeed, a signal for HSP90 α , although

TABLE 1. Cytoskeletal Marker Expression in iERMs

Antibodies	Number of Tested Samples	Number of Samples with Positive Expression
GFAP	33	29 (78.8%)
α SMA	33	32 (97%)
Vimentin	33	33 (100%)

TABLE 2. Number of iERMs with a Clear Prevalence of α SMA- or GFAP-Expressing Cells or with Approximately a Comparable Number of Two Cell Types

Antibodies	Number of Tested Samples	α SMA > GFAP	α SMA = GFAP	α SMA < GFAP
α SMA/GFAP	33	20 (60.6%)	12 (36.4%)	1 (3%)

fainter, could be observed also in GFAP⁺ cells (Fig. 3), which for the most part were α SMA[−] cells (Fig. 1). Finally, to identify cells possibly involved in ERM collagen deposition, we carried out experiments to spot intracellular type-I collagen staining that could be observed in 41.7% of samples. Triple labeling experiments characterized these cells as vimentin⁺/ α SMA⁺/HSP90 α ⁺ elements (Figs. 4A–H).

HSP90 Enhances TGF- β 1 Pathway Activation in Müller Glial Cells

To analyze the effect of HSP90 overexpression on TGF- β 1 pathway in Müller glial cells, MIO-M1 cells were transduced with lentiviruses encoding for the human FLAG-tagged HSP90 or GFP (as control) (Fig. 5A) and treated with TGF- β 1. In comparison to GFP-expressing cells, over-

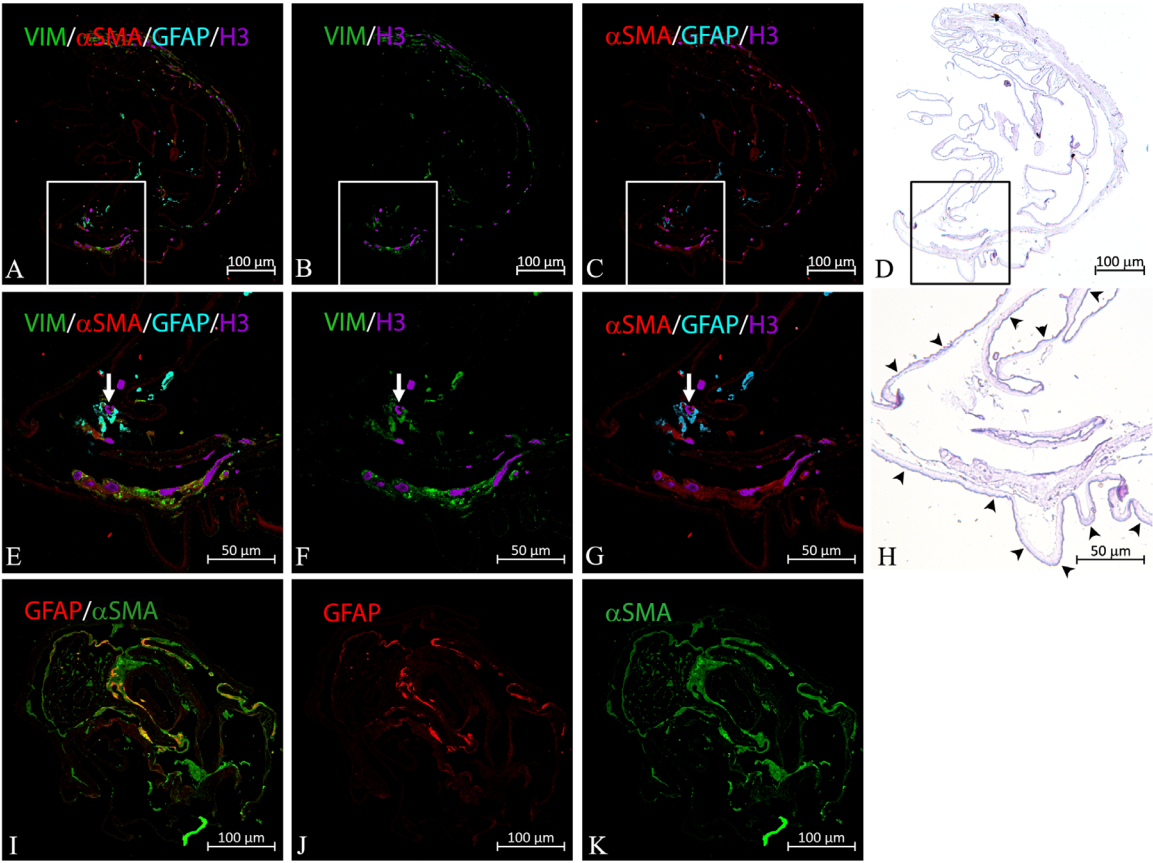


FIGURE 1. Cytoskeletal markers expressed by cells in iERMs. (A–C) Differential expression of GFAP and α SMA in vimentin⁺ cells as assessed by confocal microscopy. Cell nuclei were labeled with anti-histone H3 antibody. (D) Bright-field microscopy of the same section employed in A–C and stained with toluidine blue demonstrates the general morphology of the ERM to which the ILM is associated. (E–G) Higher magnification of the framed area in A–C; vimentin immunoreactivity mostly colocalizes with α SMA (yellowish color). The intensity of the staining for α SMA, however, is variable. Instead of α SMA, some vimentin immunoreactivity colocalizes with GFAP (arrow). (H) Higher magnification of the framed area in D. The ILM is highlighted by arrowheads. (I–K) Some GFAP/ α SMA double immunoreactivity can be also found (yellow/orange colors).

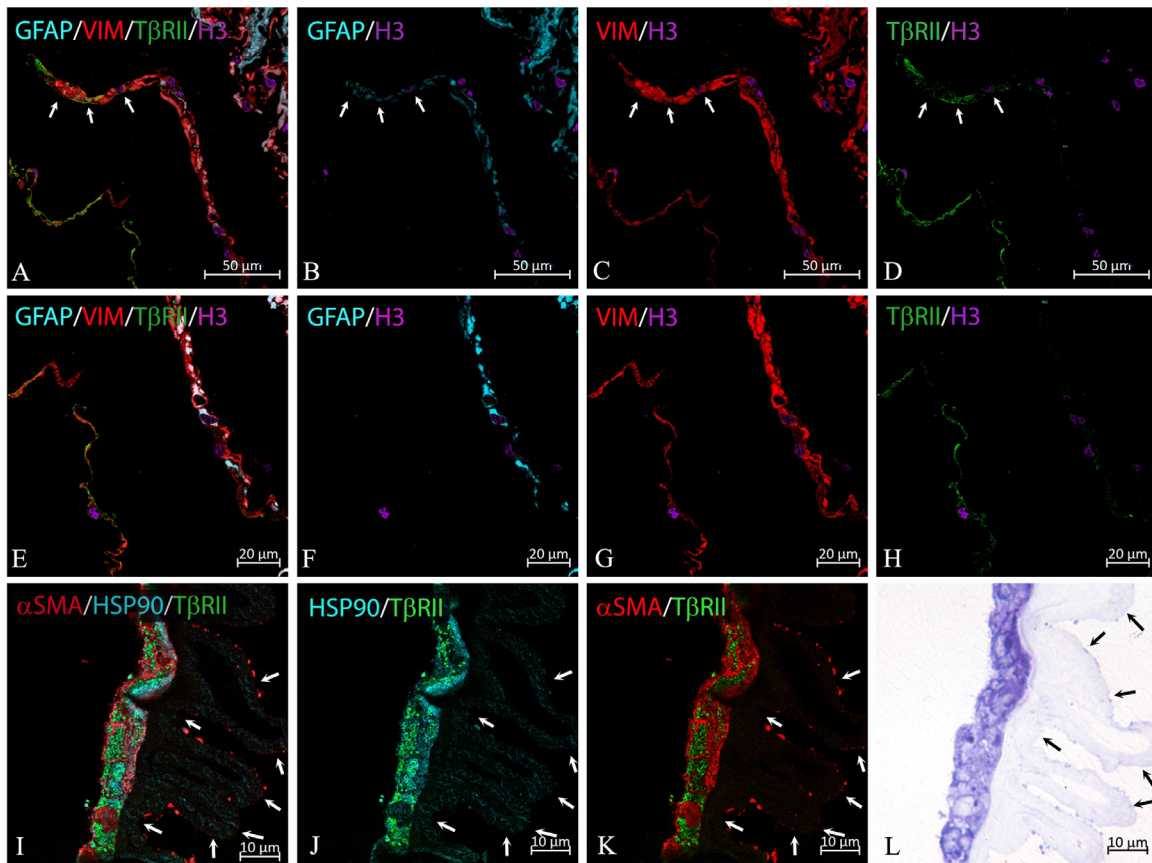


FIGURE 2. T β RII expression in iERMs. (A–D) Because of the ERM folding, confocal microscopy shows ERM cells arranged in two rows and in a larger cluster, which is also the result of membrane folding. The left row is made of vimentin⁺/GFAP[−] cells, the right row and the cluster (in the right superior corner of the figure) is formed by double-positive cells. The anti-T β RII antibody labels almost exclusively the left row of cells in the left inferior corner of the figure (vimentin⁺/GFAP[−] cells). However, few vimentin/GFAP double-positive cells are also labeled (arrows). Cell nuclei were labeled with anti-histone H3 antibody. (E–H) Higher magnification of the lower region of the field shown in A–D. T β RII immunoreactivity is almost completely restricted to the vimentin⁺/GFAP[−] cells on the left. (I–L) Confocal microscopy of cells expressing high levels of T β RII, which are also HSP90 α / α SMA double-immunoreactive cells. Arrows point to the retinal side of the ILM, which is associated with the ERM. (K) Bright-field microscopy on a toluidine blue stained consecutive section of the same area shown in I–L. The ERM is associated with the ILM (arrows points to its retinal edge), which is also visible in I and J due to a very low level of background.

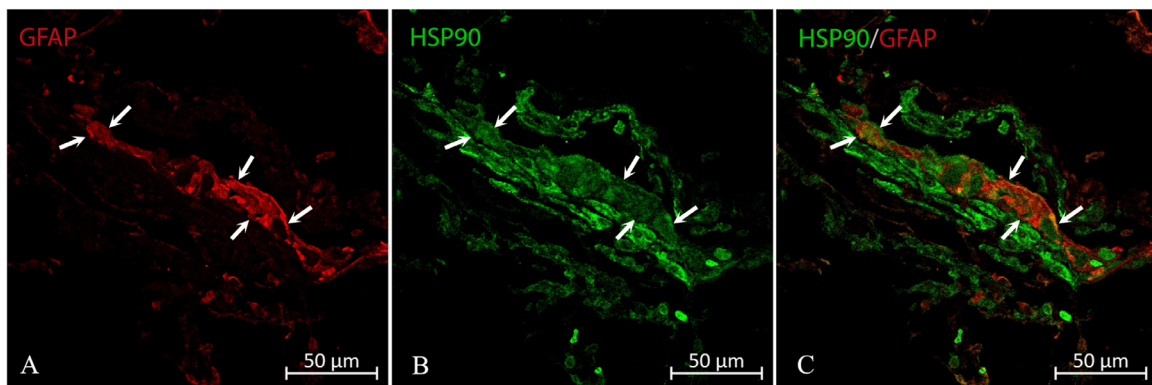


FIGURE 3. (A–C) HSP90 α differential expression in iERM. HSP90 α expression does not appear uniform in cells of iERMs. Double labeling with GFAP shows that GFAP-expressing cells (arrows) contain less HSP90 α than most GFAP⁺ cells.

expression of HSP90 resulted in an increased basal level of SMAD2, SMAD3, and TGF β RII suggesting that, in Müller glial cells, HSP90 is involved in the stabilization of all these key elements of TGF- β 1 transduction path-

way. As a consequence of this, TGF- β 1 treatment induced a higher rate of TGF- β 1 pathway activation, as demonstrated by enhanced SMAD2 phosphorylation in HSP90 overexpressing cells (Fig. 5B).

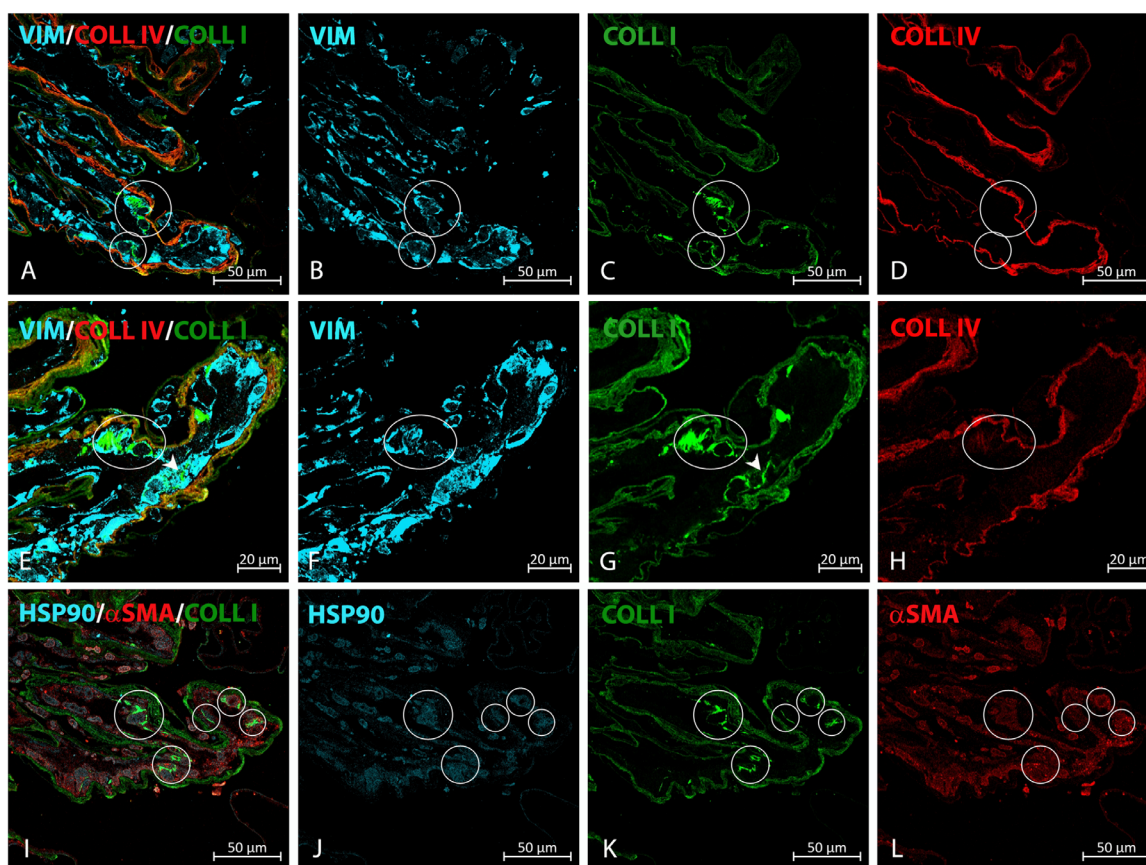


FIGURE 4. Type-I collagen intracellular staining in iERM. (A–D) Type-I collagen can be found within vimentin⁺ cells lining a type-I and type-IV collagen immunoreactive membrane. Cells with type-I collagen intracellular staining have been highlighted. (E–H) Higher magnification on a second section from the same sample shown in A–D. In E and G some cells with type-I collagen intracellular staining have been circled or pointed at with an arrowhead. (I–L) Further analysis carried out on a third section from the same sample shown in A–D shows that type-I collagen containing cells are also HSP90⁺/αSMA⁺ expressing cells. Cells with type-I collagen intracellular staining have been circled.

SMAD2 is Translocated to the Nucleus of iERM Cells

On the grounds of these results, to establish if the TGF-β1-induced transduction pathway was actually activated *in vivo*, we carried out additional immunofluorescence experiments on frozen sections of iERMs. Sections immunolabeled with anti-SMAD2 and anti-HSP90α antibodies showed both cytoplasmic and nuclear staining for SMAD2 either in HSP90α⁺ or HSP90α⁻ cells and some HSP90α⁺ cells that were devoid of SMAD2 nuclear labeling. At any rate, some HSP90α-expressing cells showed SMAD2 nuclear staining confirming that, at least in some cells, SMAD2 translocated to the nucleus (Fig. 6).

DISCUSSION

Patients affected by iERM may be asymptomatic or have serious visual impairment. In-between these two extreme conditions, a continuum of different degrees of severity can be observed.¹ Only in the United States, approximately 30 million individuals are estimated to have at least one eye affected with an iERM.³⁴ Idiopathic vitreoretinal proliferation (i.e., iERM) is therefore a major visual-threatening eye disorder, and any investigation that aids to shed some light on the physiopathology underlying its development may be

important to devise new therapies or to perfect already existing treatments.

Bearing this in mind, we began our investigation to characterize cells in iERMs employing a novel approach, which has been previously applied to ERMs only once.²² In short, it consists of processing and embedding samples for electron microscopy and cutting 1-μm thick resin sections that were subsequently employed for immunofluorescence microscopy. The number of antibodies that can be used with this technique is higher than expected because of the recently devised improved heat-induced antigen retrieval procedures.³⁵ We chose this approach as we wanted to carry out a large number of reactions on the same iERMs, which are notoriously very small samples.

We started using basic markers, such as intermediate filaments (vimentin and GFAP) and αSMA. Our results, being substantially in agreement with previous studies,⁷ confirm the reliability of the technique and show that two major populations of cells can be found in iERMs: one is formed by GFAP⁺/αSMA⁻ cells, the other by GFAP⁻/αSMA⁺ cells. A minor population of GFAP⁺/αSMA⁺ can also be observed but it consists of very few and scattered cells. In general, membranes with a majority of GFAP⁺ cells were poor in αSMA⁺ cells and, vice-versa, membranes with a majority of αSMA⁺ cells were poor in GFAP⁺ cells. However, virtually all cells express vimentin. These results suggest that

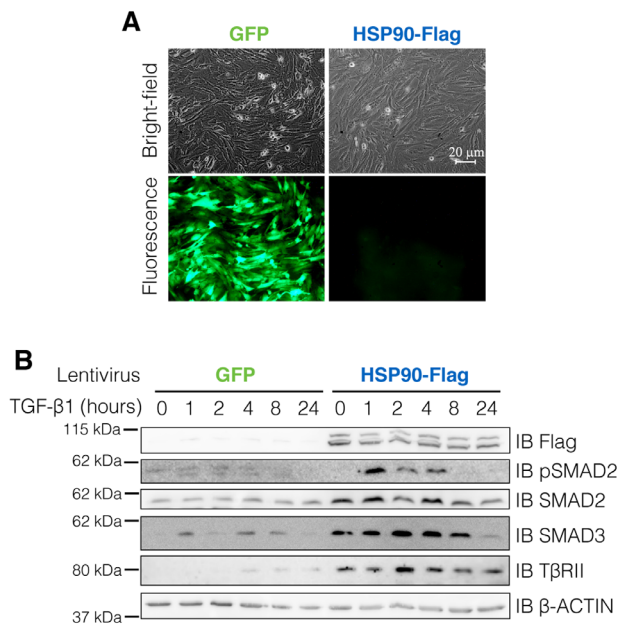


FIGURE 5. HSP90 enhances SMAD2, SMAD3, and TβRII expression and TGF-β1 pathway activation in Müller glial cells. **(A)** MIO-M1 Müller glia cells were transduced with lentiviruses encoding for the human FLAG-tagged HSP90 or GFP (as control). Transduction efficiency was monitored by fluorescence microscopy analysis of GFP expression in control cells. **(B)** Transduced cells were treated with human recombinant TGF-β1. Expression of endogenous SMAD2, SMAD3, and TGFβRII and transduced FLAG-tagged HSP90 were analyzed by immunoblot. TGF-β1 pathway activation was assayed using a specific phospho-SMAD2 (Ser465/467) antibody. The expression of β-actin was used as loading protein control.

a population of GFAP⁺/αSMA⁻ cells is capable of moving to the vitreoretinal interface and transdifferentiate toward an αSMA⁺ myofibroblast-like cell phenotype. The rarity of GFAP⁺/αSMA⁺ cells also suggests that once the cells start to transdifferentiate toward the αSMA⁺ myofibroblastic phenotype they rapidly lose GFAP. As GFAP in the retina is expressed only by astrocytes and, on activation, also by Müller cells,³⁶ it is reasonable to hypothesize that most of the cells in iERMs may derive by one or both of these cell types. Actually, GFAP-immunoreactive Müller cells have been previously caught traversing the ILM and extending into ERMs.³⁷

It has been reported that iERMs contain cells expressing TβRII.⁷ This is significant as TGF-β seems to be an important player in several macular diseases. For instance, in addition to TGF-β1 in cells within iERMs,⁷ high levels of TGF-β2 have been also detected in the vitreous of patients affected by the same pathology and by neovascular age-related macular degeneration.^{38–40}

However, a more detailed characterization of TβRII-expressing cells lacked. Here we have shown that TβRII-expressing cells are GFAP⁻/vimentin⁺/αSMA⁺ cells.

Considering that only few TβRII⁺ cells coexpress GFAP and vimentin, it is possible that these cells, such as GFAP⁺/αSMA⁺ cells, might represent glial cells in the early stages of transdifferentiation.

To further characterize TβRII⁺ cells, we have also shown that these cells express HSP90α and that TβRII⁺/HSP90α⁺/αSMA⁺ cells contain type-I collagen, suggesting that they are likely responsible for collagen deposition. Our experiments did demonstrate HSP90α in most but not all iERMs.

This is probably because of the antibody employed in this study, which is specific for the alpha isoform of HSP90 that, in contrast to the constitutively expressed HSP90β, is an inducible isoform.⁴¹ Indeed, the inducible nature of HSP90α also explains why its expression does not appear uniform even within the same iERM, being usually less evident in GFAP⁺ cells.

HSP90α higher level of expression in TβRII⁺/αSMA⁺ cells prompted us to investigate its putative role in the development of the ERMs in vitro using the spontaneously immortalized Müller cell line MIO-M1. We chose this cell line as there is evidence that at least part of ERM cells may derive from Müller cells as previously reported.⁹ Our results show that HSP90 overexpression changes substantially TGF-β1-induced signal transduction pathway with an increased expression of TβRII⁺, SMAD2, and SMAD3 and with enhanced levels of SMAD2 phosphorylation. TGF-β1, previously reported in iERMs,⁷ can therefore activate SMAD2/3 intracellular transduction pathway more efficiently when cells express HSP90. It is well known that TGF-β1 is a profibrotic cytokine. It increases αSMA protein expression and type-I collagen synthesis by binding to TβRII and activating the SMAD pathway, which is crucial for tissue fibrosis.²⁴ This pathway is partially quenched by Smurf-dependent TβRII ubiquitination, which directs the receptor to the proteasome system.⁴² As HSP90 is capable of protecting TβRII from proteasome degradation, it is also able to prolong TβRII phosphorylating activity, to maintain active the SMAD pathway and to increase TGF-β1 target gene expression.⁴³ Thus HSP90 enhances the profibrotic weight of TGF-β1. Our finding that SMAD2 is translocated to the nucleus of HSP90⁺ even in vivo suggests that the well-established mechanisms underlying TGF-β1-induced matrix deposition in several fibrotic diseases^{44–47} likely operate in iERMs as well. The use of Epon-embedded samples in this research has certainly reached the goal to allow us to make several different reactions on the same samples and gather more information from the same iERM. In addition, glutaraldehyde fixation and osmium post-fixation achieved a high level of tissue preservation unveiling many structural details that more conventional approaches could have missed. However, this technique has its drawbacks that also represent the limit of the present study. In particular, we could not use regular DNA dyes that do not work with such a strong fixation and on the harsh procedures required to deplastize sections and to retrieve antigenicity (121°C). Moreover, although many antibodies have been successfully employed in this study, many others fail to bind their antigens in our setting despite that they are known to work with more conventional immunohistochemical approaches (i.e., formalin-fixed paraffin embedded samples). For instance, a convincing labeling of the ILM could not be achieved, although we tried several antibodies against the components of the membrane. Nevertheless, we could achieve a deeper characterization of αSMA⁺ myofibroblast-like cells that resulted in GFAP⁻/αSMA⁺/vimentin⁺/HSP90α⁺ and in almost half of the cases contained type-I collagen. The positive effects of HSP90 on the activation of the TGF-β1-induced SMAD-dependent transduction pathway has also been confirmed in vitro with HSP90-overexpressing MIO-M1 cells.

Because of the difficulties in collecting and processing ERMs, the number of samples we employed appears adequate for a study carried out mainly by immunofluorescence and confocal microscopy. However, more samples

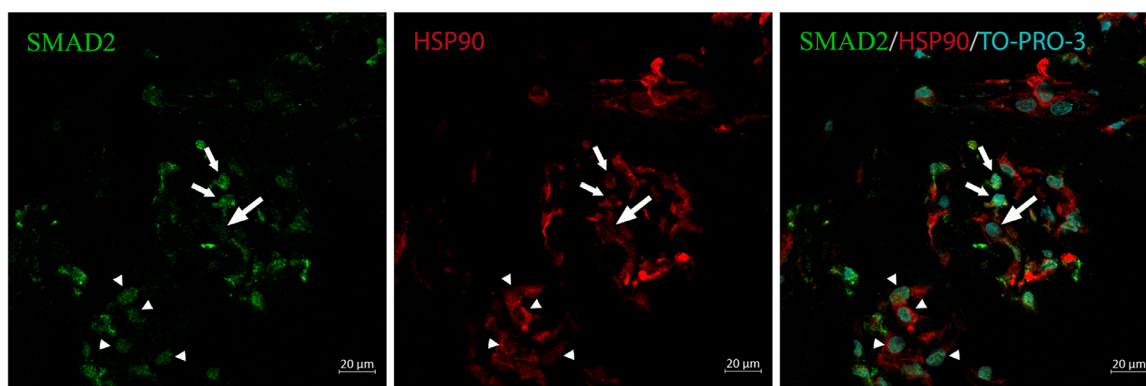


FIGURE 6. SMAD2 translocation to the nucleus of iERM cells. Frozen sections were immunostained with anti-SMAD2 and anti-HSP90 α antibody. Nuclei were counterstained with TO-PRO-3 iodide. Some HSP90 α ⁺ cells have only a faint SMAD2 cytoplasmic fluorescence (*large arrow*), some cells show only SMAD2 nuclear staining (*arrowheads*), and some HSP90 α ⁺ cells show SMAD2 cytoplasmic and nuclear staining (*small arrows*). SMAD2 nuclear staining indicates activation of the SMAD pathway.

are needed to evaluate any correlation between the different cellular components and the clinical characteristics.

CONCLUSIONS

Although more studies are needed, on the grounds of our observations we propose to consider HSP90 as a potential therapeutic target for iERMs.

Acknowledgments

The authors thank G.A. Limb (Institute of Ophthalmology and Moorfields Eye Hospital) for providing the MIO-M1 cell line, and D. Orazioli for her excellent technical assistance.

Supported by MIUR (Ministero dell'Istruzione, dell'Università e della Ricerca) Grant "Dipartimento di eccellenza 2018-2022" to the Department of Biotechnology, Chemistry and Pharmacy, and by the I.Ri.Fo.R Onlus (Institute for the Research, Formation and Rehabilitation) Italian Union of Blind and Visually Impaired People.

Disclosure: **G.M. Tosi**, None; **M. Regoli**, None; **A. Altera**, None; **F. Galvagni**, None; **C. Arcuri**, None; **T. Bacci**, None; **I. Elia**, None; **G. Realini**, None; **M. Orlandini**, None; **E. Bertelli**, None

References

- Folk JC, Adelman RA, Flaxel CJ, Hyman L, Pulido JS, Olsen TW. Idiopathic epiretinal membrane and vitreomacular traction preferred practice pattern guidelines. *Ophthalmology*. 2016;123:P152–P181.
- Foss RY. Vitreoretinal juncture; epiretinal membranes and vitreous. *Invest Ophthalmol Vis Sci*. 1977;16:416–422.
- Oberstain SY, Byun J, Herrera D, Chapin EA, Fisher SK, Lewis GP. Cell proliferation in human epiretinal membranes: characterization of cell types and correlation with disease condition and duration. *Mol Vis*. 2011;17:1794–1805.
- Zhao F, Gandorfer A, Haritoglou C, et al. Epiretinal cell proliferation in macular pucker and vitreomacular traction syndrome. Analysis of flat-mounted internal limiting membrane specimens. *Retina*. 2013;33:77–88.
- Schumann RG, Eibl KH, Zhao F, et al. Immunocytochemical and ultrastructural evidence of glial cells and hyalocytes in internal limiting membrane specimens of idiopathic macular holes. *Invest Ophthalmol Vis Sci*. 2011;52:7822–7834.
- Hiscott PS, Grierson I, McLeod D. Natural history of fibrocellular epiretinal membranes: a quantitative, autoradiographic, and immunohistochemical study. *Br J Ophthalmol*. 1985;69:810–823.
- Bochaton-Piallat M-L, Kapetanios AD, Donati G, Redard M, Gabbiani G, Pournaras CJ. TGF β 1, TGF β receptor II and ED-A fibronectin expression in myofibroblast of vitreoretinopathy. *Invest Ophthalmol Vis Sci*. 2000;41:2336–2342.
- Schumann RG, Gandorfer A, Ziada J, et al. Hyalocytes in idiopathic epiretinal membranes: a correlative light and electron microscopic study. *Graefes Arch Clin Exp Ophthalmol*. 2014;52:1887–1894.
- Bu S-C, Kuijer R, van der Worp RJ, et al. Immunohistochemical evaluation of idiopathic epiretinal membranes and in vitro studies on the effect of TGF β on Müller cells. *Invest Ophthalmol Vis Sci*. 2015;56:6506–6514.
- Tamiya S, Kaplan HJ. Role of epithelial-mesenchymal transition in proliferative vitreoretinopathy. *Exp Eye Res*. 2016;142:26–31.
- Grisanti S, Guidry C. Transdifferentiation of retinal pigment epithelial cells from epithelial to mesenchymal phenotype. *Invest Ophthalmol Vis Sci*. 1995;36:391–405.
- Tamiya S, Liu L, Kaplan HJ. Epithelial-mesenchymal transition and proliferation of retinal pigment epithelial cells initiated upon loss of cell-cell contact. *Invest Ophthalmol Vis Sci*. 2010;51:2755–2763.
- Limb GA, Salt TE, Munro PMG, Moss SE, Khaw PT. In vitro characterization of a spontaneously immortalized human Müller cell line (MIO-M1). *Invest Ophthalmol Vis Sci*. 2002;43:864–869.
- Zhang X, Feng Z, Li C, Zheng Y. Morphological and migratory alterations in retinal Müller cells during early stages of hypoxia and oxidative stress. *Neural Regen Res*. 2012;7:31–35.
- Kanda A, Noda K, Hirose I, Ishida S. TGF- β -SNAIL axis induces Müller glial-mesenchymal transition in the pathogenesis of idiopathic epiretinal membrane. *Sci Rep*. 2019;9:673.
- Moreels M, Vandenabeele F, Dumont D, Robben J, Lambrechts I. Alpha-smooth muscle actin (alpha-SMA) and nestin expression in reactive astrocytes in multiple sclerosis lesions: potential regulatory role of transforming

- growth factor-beta 1 (TGF-beta1). *Neuropathol Appl Neurobiol.* 2008;34:532–546.
17. Jerdan JA, Pepose JS, Michels RG, et al. Proliferative vitreoretinopathy membranes. An immunohistochemical study. *Ophthalmology.* 1989;96:801–810.
 18. Immonen I, Tervo K, Virtanen I, Laatikainen L, Tervo T. Immunohistochemical demonstration of cellular fibronectin and tenascin in human epiretinal membranes. *Acta Ophthalmol.* 1991;69:466–471.
 19. Hagedorn M, Esser P, Wiedemann P, Heimann K. Tenascin and decorin in epiretinal membranes of proliferative vitreoretinopathy and proliferative diabetic retinopathy. *German J Ophthalmol.* 1993;2:28–31.
 20. Kritzenberger M, Junglas B, Framme C, et al. Different collagen types define two types of idiopathic epiretinal membranes. *Histopathology.* 2011;58:953–965.
 21. Bu SC, Kuijter R, van der Worp RJ, et al. Glial cells and collagens in epiretinal membranes associated with idiopathic macular holes. *Retina.* 2014;34:897–906.
 22. Regoli M, Tosi GM, Neri G, Altera A, Orazioli D, Bertelli E. The peculiar pattern of type IV collagen deposition in epiretinal membranes. *J Histochem Cytochem.* 2020;68:149–162.
 23. Friedman SL, Sheppard D, Duffield JS, Violette S. Therapy for fibrotic diseases: nearing the starting line. *Sci Transl Med.* 2013;5:167sr1.
 24. Hu H-H, Chen D-Q, Wang Y-N, et al. New insights into TGF- β /Smad signaling in tissue fibrosis. *Chem Biol Interact.* 2018;292:76–83.
 25. Szeto SG, Narimatsu M, Lu M, et al. YAP/TAZ are mechanoregulators of TGF- β -Smad signaling and renal fibrogenesis. *J Am Soc Nephrol.* 2016;27:3117–3128.
 26. Myung SJ, Yoon J-H, Kim BH, Lee J-H, Jung EU, Lee H-S. Heat shock protein 90 inhibitor induces apoptosis and attenuates activation of hepatic stellate cells. *J Pharmacol Exp Therap.* 2009;330:276–282.
 27. Noh H, Kim HJ, Yu MR, et al. Heat shock protein 90 inhibitor attenuates renal fibrosis through degradation of transforming growth factor- β type II receptor. *Lab Invest.* 2012;92:1583–1596.
 28. Dong H, Luo L, Zou M, et al. Blockade of extracellular heat shock protein 90 α by 1G6-D7 attenuates pulmonary fibrosis through inhibiting ERK signaling. *Am J Physiol Lung Cell Mol Physiol.* 2017;313:L1006–L1015.
 29. Sontake V, Wang Y, Kasam RK, et al. HSP90 regulation of fibroblast activation in pulmonary fibrosis. *JCI Insight.* 2017;2:e91454.
 30. Di Bella A, Regoli M, Nicoletti C, Ermini L, Fonzi L, Bertelli E. An appraisal of intermediate filament expression in adult and developing pancreas: vimentin is expressed in α cells of rat and mouse embryos. *J Histochem Cytochem.* 2009;57:577–586.
 31. Hartig R, Haung Y, Janetzko A, Shoeman R, Grüb S, Traub P. Binding of fluorescence- and gold-labeled oligodeoxyribonucleotides to cytoplasmic intermediate filaments in epithelial and fibroblast cells. *Exp Cell Res.* 1997;233:169–186.
 32. Galvagni F, Lentucci C, Neri F, et al. Snai1 promotes ESC exit from the pluripotency by direct repression of self-renewal genes. *Stem Cells.* 2015;33:742–750.
 33. Anselmi F, Orlandini M, Rocchigiani M, et al. c-ABL modulates MAP kinases activation downstream of VEGFR-2 signaling by direct phosphorylation of the adaptor proteins GRB2 and NCK1. *Angiogenesis.* 2012;15:187–197.
 34. Klein R, Klein BEK, Wang Q, Moss SE. The epidemiology of epiretinal membranes. *Tr Am Ophthalmol Soc.* 1994;92:403–430.
 35. Yamashita S, Okada Y. Heat-induced antigen retrieval in conventionally processed epon-embedded specimens: procedures and mechanisms. *J Histochem Cytochem.* 2014;62:584–597.
 36. Luna G, Laewi GP, Banna CD, Skalli O, Fisher SK. Expression profiles of nestin and synemin in reactive astrocytes and Müller cells following retinal injury: a comparison with glial fibrillary acidic protein and vimentin. *Mol Vis.* 2010;16:2511–2535.
 37. Fisher SK, Lewis GP. Müller cells and neuronal remodeling in retinal detachment and reattachment and their potential consequences for visual recovery: a review and reconsideration of recent data. *Vis Res.* 2003;43:887–897.
 38. Minchiotti S, Stampachiachiere B, Micera A, et al. Human idiopathic epiretinal membranes express NGF and NGF receptors. *Retina.* 2008;28:628–637.
 39. Ishikawa K, Yoshida S, Nakao S, et al. Periostin promotes the generation of fibrous membranes in proliferative vitreoretinopathy. *FASEB J.* 2014;28:131–134.
 40. Tosi G M, Neri G, Caldi E, et al. TGF- β concentrations and activity are down-regulated in the aqueous humor of patients with neovascular age-related macular degeneration. *Sci Rep.* 2018;8:8053.
 41. Sredhaar AS, Kalmar E, Csermely P, Shen Y-F. HSP90 isoforms: functions, expression and clinical importance. *FEBS Lett.* 2004;562:11–15.
 42. Kavsak R, Rasmussen RK, Causing CG, et al. Smad7 binds to Smurf2 to form an E3 ubiquitin ligase that targets the TGF beta receptor for degradation. *Mol Cell.* 2000;6:1365–1375.
 43. Wrighton KH, Lin X, Feng XH. Critical regulation of TGF β signalling by HSP90. *Proc Natl Acad Sci USA.* 2008;105:9244–9249.
 44. Li M, Krishnaveni MS, Li C, et al. Epithelium-specific deletion of TGF- β receptor type II protects mice from bleomycin-induced pulmonary fibrosis. *J Clin Invest.* 2011;121:277–287.
 45. Lunghi B, De Cunto G, Cavarra E, et al. Smoking p66Shc knocked out mice develop respiratory bronchiolitis with fibrosis but not emphysema. *PLoS One.* 2015;10:e0119797.
 46. Meng XM, Nikolic-Paterson DJ, Lan HY. TGF- β : the master regulator of fibrosis. *Nat Rev Nephrol.* 2016;12:325–338.
 47. Walton KL, Johnson KE, Harrison CA. Targeting TGF- β mediated SMAD signaling for the prevention of fibrosis. *Front Pharmacol.* 2017;8:461.